Nuclear structure theory in spin- and number-conserving quasiparticle configuration spaces: First applications

K. W. Schmid,[a] F. Grümmer,[b] and Amand Faessler[a]
(a) Institut für Theoretische Physik, Universität Tübingen, D-7400 Tübingen, Federal Republic of Germany
(b) Institut für Kernphysik, Kernforschungsanlage Jülich, D-5170 Jülich, Federal Republic of Germany
(Received 21 March 1983)

In the first part of the present series of two papers we discussed several nuclear structure models all working in configuration spaces consisting of spin- and number-projected quasiparticle determinants. In the present paper a particular version of the numerically simplest of these models is presented. This model approximates the nuclear wave functions by linear combinations of the angular momentum- and particle number-projected Hartree-Fock-Bogoliubov vacuum and the equally spin- and number-projected two quasiparticle excitations with respect to it. The model allows the use of realistic two body interactions and rather large model spaces. It can hence be applied to a large number of nuclear structure problems in various mass regions. First applications have been performed for the nuclei ^{20}Ne, ^{22}Ne, ^{46}Ti, and ^{164}Er. In all these cases the results are very encouraging.

[NUCLEAR STRUCTURE ^{20}Ne, ^{22}Ne, ^{46}Ti, ^{164}Er; calculated spectra and transitions. Spin- and number-projected Hartree-Fock-Bogoliubov and shell model methods.]

I. INTRODUCTION

In the first part[1] of the present series of two papers (hereafter referred to as I) we have given a general survey about the mathematical formalism, which is necessary to perform microscopic nuclear structure calculations in configuration spaces consisting of arbitrary angular momentum- and particle-number-projected Hartree-Fock-Bogoliubov—type (HFB-type) quasiparticle determinants. On the basis of this formalism we have then discussed several possible nuclear structure models differing essentially by the degree of sophistication with which the configuration spaces and the corresponding mean HFB fields were optimized.

In the present paper we shall now concentrate on the simplest version of these models (the "fourth best" approach to the problem according to I), which uses a spin- and configuration-space-independent mean field obtained by a standard HFB calculation as reference to construct all the quasiparticle determinants to be taken into account. If we furthermore specialize the configuration spaces to include only the angular-momentum- and particle-number-projected HFB vacuum [the "zero-quasiparticle" (0qp) determinant] and the equally spin- and number-projected corresponding two-quasiparticle (2qp) excitations, we obtain the MONSTER approach (model for handling large numbers of number- and spin-projected two quasiparticle excitations with realistic interactions and model spaces), which was first presented in some conferences[2] and will be described in detail in the following sections. First steps in the direction of such a theory had already been made long ago[3] and have found some new interest in the last couple of years[4,5] before the first general applications can now be presented.

In Sec. II we shall first discuss the essential additional approximations which had to be introduced in order to make the MONSTER a numerically feasible method. This section will also describe how possible spurious admixtures due to the center-of-mass motion can be at least approximately eliminated and will furthermore discuss the advantages of the MONSTER approach as compared to some other nuclear structure models. Section III will then give a brief description of the numerical procedure of a MONSTER calculation and discuss the possibilities and limitations of the presently existing computer code. In Sec. IV then the results of first applications will be presented. There we shall start with a small basis system ($1s\,0d$ shell), in which complete shell model diagonalizations of given effective many nucleon Hamiltonians can still be performed. Comparison of the MONSTER results with such "exact" solutions will provide a crucial test for the quality of our approximations. As examples here the cases of ^{20}Ne and ^{22}Ne will be considered. We shall then proceed to a larger basis system ($1p\,0f$ shell) and study the nucleus ^{46}Ti. Since for this nucleus to our knowledge no complete shell model diagonalization within the full pf space has been performed, we shall compare our results here with those of other approximate methods and with the experimental data. Finally, we shall use an even larger single particle basis ($N=4+0h_{9/2}+0h_{11/2}$ for protons; $N=5+1g_{9/2}+0i_{13/2}$ for neutrons) to perform calculations for the nucleus ^{164}Er. There the spectra as well as the corresponding $B(E2)$ values will be compared again with the experimental data. In Sec. V we shall then summarize our first experiences with the MONSTER and discuss some further applications and possible improvements.

II. THE MONSTER APPROXIMATIONS

We start by assuming that the single-particle basis consists of M_p proton and M_n neutron eigenstates of some spherical basis creating potential, for example, a harmonic oscillator or a Woods-Saxon well. Coulomb, spin-orbit, and l^2 terms may or may not be included. Denoting the particle vacuum by $|0\rangle$, each basis orbit $|i\rangle$ and the corresponding creation and annihilation operators $C_i^\dagger$ and C_i can then be characterized by the quantum numbers

$$|i\rangle \equiv C_i^\dagger |0\rangle = |\tau_i n_i l_i j_i m_i\rangle , \tag{1}$$

where τ_i gives the isospin projection of the orbit ($-\frac{1}{2}$ or $\frac{1}{2}$ for a proton or a neutron orbit, respectively), l_i is its orbital and j_i its total angular momentum, m_i measures the projection of j_i along the chosen quantization axis, and n_i distinguishes between the different radial wave functions, which in general may still depend on the other quantum numbers. Since for each j_i all the $2j_i+1$ magnetic substates ($-j_i \le m_i \le j_i$) will always be included, M_p and M_n are both positive even integers. We shall furthermore assume that the effective many nucleon Hamiltonian appropriate for the chosen basis system is known, can be written as a sum of only one- and two-body terms

$$\hat{H} = \sum_{ir} t(ir) C_i^\dagger C_r + \tfrac{1}{4} \sum_{ikrs} v(ikrs) C_i^\dagger C_k^\dagger C_s C_r , \tag{2}$$

and that the matrix elements of the one-body term $t(ir) \equiv \langle i | \hat{t} | r \rangle$ as well as the antisymmetrized two-body matrix elements of the effective nucleon-nucleon interaction $v(ikrs) \equiv \langle ik | \hat{V} | rs - sr \rangle$ are all real numbers as can always be guaranteed provided the phases of the basis orbits are suitably chosen.

Within the model space spanned by the basis states (1) the general HFB transformation[6] then has the form

$$a_\alpha^\dagger(q) \equiv \sum_i \{A_{i\alpha}(q) C_i^\dagger + B_{i\alpha}(q) C_i\} , \tag{3}$$

where the sum runs in principle over all the quantum numbers of the spherical basis and the index q distinguishes as in I between different quasiparticle transformations of the type (3).

The first essential approximation being introduced now is the neglect of the parity mixing in the transformation (3). Consequently, the quasiparticle orbits (3) as well as all the quasiparticle determinants constructed from them are then eigenstates of the parity operator. As second approximation we shall assume that (3) does not mix basis states with different isospin projections. This assumption is equivalent to the neglect of proton-neutron pairing in the mean HFB field and seems to be rather well justified at least as far as neutron excess nuclei are considered.[7] Besides the restriction of the sum in Eq. (3) to either proton or neutron states this approximation has the additional advantage that the transformation matrices $A(q)$ and $B(q)$ can both be chosen real. Finally, as a third approximation, we shall impose axial symmetry on the transformation (3). Thus all the quasiparticle states (3) and hence obviously also all the resulting quasiparticle determinants will be eigenstates of the z component of the total spin operator acting in the intrinsic space. As we shall see in the following this last approximation leads to drastic simplifications in the calculation of the angular momentum projected matrix elements.

With the above assumptions the transformation (3) can now be written as

$$a_\alpha^{\tau_\alpha \pi_\alpha m_\alpha \dagger}(q) \equiv \sum_{\substack{\tau_i n_i l_i j_i \\ m_i > 0}} \delta(\tau_i,\tau_\alpha)\delta((-)^{l_i},\pi_\alpha)\delta(m_i,m_\alpha)\{A_{i\alpha}^{\tau_\alpha \pi_\alpha m_\alpha}(q) C_i^\dagger - B_{i\bar{\alpha}}^{\tau_\alpha \pi_\alpha m_\alpha}(q) C_{\bar{i}}\} \tag{4}$$

and

$$a_{\bar{\alpha}}^{\tau_\alpha \pi_\alpha -m_\alpha \dagger}(q) \equiv \sum_{\substack{\tau_i n_i l_i j_i \\ m_i > 0}} \delta(\tau_i,\tau_\alpha)\delta((-)^{l_i},\pi_\alpha)\delta(m_i,m_\alpha)\{A_{i\alpha}^{\tau_\alpha \pi_\alpha m_\alpha}(q) C_{\bar{i}}^\dagger + B_{i\bar{\alpha}}^{\tau_\alpha \pi_\alpha m_\alpha}(q) C_i\} , \tag{5}$$

where a bar as usual denotes the time reversed partner of a particular state using the phase convention

$$|\bar{i}\rangle \equiv \hat{\tau} |i\rangle = (-)^{l_i + j_i - m_i} |\tau_i n_i l_i j_i - m_i\rangle \tag{6}$$

with $\hat{\tau}$ being the time reversal operator. Furthermore, in Eqs. (4) and (5) use has been made of the relations

$$A_{i\bar{\alpha}} = -A_{\bar{i}\alpha} = B_{i\alpha} = B_{\bar{i}\bar{\alpha}} = 0 \tag{7}$$

and

$$A_{i\alpha} = A_{\bar{i}\bar{\alpha}}, \quad B_{\bar{i}\alpha} = -B_{i\bar{\alpha}} , \tag{8}$$

where m_i and m_α are both supposed to be positive.

The HFB vacuum serving in the following as reference determinant can then be written as

$$|\{q\}_0\rangle \equiv \prod_{\alpha>0} a_\alpha(q) a_{\bar{\alpha}}(q) |0\rangle , \tag{9}$$

where $\alpha > 0$ restricts the product to the $(M_p + M_n)/2$ states with $m_\alpha > 0$. Because M_p and M_n are both even and the proton-neutron pairing has been neglected, the zero-quasiparticle (0qp) determinant (9) contains only components corresponding to even proton and neutron numbers. Furthermore, it has positive parity, total angular momentum projection $K_0 = 0$ along the intrinsic z axis, and is even under time reversal. Consequently a general n-quasiparticle ($n$qp) excitation with respect to (9)

$$|\{q\} q_1 q_2 \cdots q_n\rangle \equiv \left[\prod_{i=1}^{n} a_{q_i}^\dagger(q) \right] |\{q\}_0\rangle \tag{10}$$

has the parity $\pi_{q_1\cdots q_n}=\pi_{q_1}\pi_{q_2}\cdots\pi_{q_n}$ and the total spin projection

$$K_{q_1\cdots q_n}=\sum_{i=1}^{n} m_{q_i} .$$

Depending on whether (10) contains an even or an odd number of proton (or neutron) quasiparticles it consists only of even or of odd proton (or neutron) number components. In the following we shall restrict ourselves to doubly even nuclei. This implies that only those n-quasiparticle states (10) consisting of an even number of proton quasiparticles ($n_p=0,2,\ldots$) and an even number of neutron quasiparticles ($n_n=0,2,\ldots$) will contribute ($n_p+n_n=n$). Extensions of the method to odd or doubly odd nuclei are easily possible but will not be discussed in the present paper.

The final approximation made in the MONSTER approach is now to truncate the complete configuration space consisting out of the reference determinant (9) and all the $n$qp excitations (10) ($n=1,\ldots,M_p+M_n$) to only the 0qp state (9) and the 2qp configurations

$$|\{q\}q_1q_2\rangle\equiv a^\dagger_{q_1}(q)a^\dagger_{q_2}(q)\,|\{q\}_0\rangle \tag{11}$$

having $\tau_{q_1}=\tau_{q_2}$.

Using the well-known number- and spin-projection operators[8,9]

$$\hat{Q}(N_0^\tau)\equiv\frac{1}{2\pi}\int_0^{2\pi} d\phi_\tau \exp\{i\phi_\tau[N_0^\tau-\hat{N}^\tau]\} \tag{12}$$

with $\hat{N}^{+1/2}\equiv\hat{N}$ being the neutron and $\hat{N}^{-1/2}\equiv\hat{Z}$ being the proton number operators and

$$\hat{P}(IM;K)\equiv\frac{2I+1}{8\pi^2}\int_{(4\pi)} d\Omega\, D^{I*}_{MK}(\Omega)\hat{R}(\Omega) \tag{13}$$

with $\hat{R}(\Omega)$ being the rotation operator[10] and $D^I_{MK}(\Omega)$ its representation in angular momentum eigenstates we may now proceed to restore the required proton and neutron numbers Z_0 and N_0 as well as the desired total angular momentum I and its projection M in the laboratory frame of reference. Thus we obtain from (9)

$$|\{q\}_0;Z_0N_0I^\pi M\rangle\equiv\delta(\pi,+)\delta((-)^I,+1)\hat{P}(IM;0)\hat{Q}(N_0)\hat{Q}(Z_0)\,|\{q\}_0\rangle \tag{14}$$

while the set of configurations resulting from (11) can be written as

$$\begin{aligned}|\{q\}q_1q_2;Z_0N_0I^\pi M\rangle\equiv{}&\delta(\pi_{q_1}\pi_{q_2},\pi)\delta(\tau_{q_1},\tau_{q_2})\delta(|m_{q_1}+m_{q_2}|\le I)\hat{Q}(N_0)\hat{Q}(Z_0)\\&\times\frac{1}{\sqrt{2}}\{\hat{P}(IM;m_{q_1}+m_{q_2})a^\dagger_{q_1}(q)a^\dagger_{q_2}(q)\\&+\pi(-)^{I-(m_{q_1}+m_{q_2})}\hat{P}(IM;-m_{q_1}-m_{q_2})a^\dagger_{\bar{q}_1}(q)a^\dagger_{\bar{q}_2}(q)\}\,|\{q\}_0\rangle\end{aligned} \tag{15}$$

if use is made from the time reversal properties of the set of 2qp configurations (11).

Owing to our above assumptions about the HFB transformation the reduced matrix element of a general tensor operator $T^{L\pi}_\mu(\Delta Z_0,\Delta N_0)$ changing the nucleon numbers by ΔZ_0 and ΔN_0, respectively, in between two arbitrary projected 2qp states of the type (15), which in general may even belong to different quasiparticle transformations q and q', gets a much simpler form than the general expression given in I. Performing two of the three integrations induced by the spin projector (13) analytically, which is possible since we have imposed axial symmetry on the quasiparticle transformation (3), and using the time reversal properties of the configurations (15) as well as the fact that they contain only even proton and neutron number components we obtain

$$\begin{aligned}&\langle\{q\}q_1q_2;Z_0+\Delta Z_0N_0+\Delta N_0I_f^{\pi_f}||\hat{T}^{L\pi}(\Delta Z_0,\Delta N_0)||\{q'\}q_1'q_2';Z_0N_0I_i^{\pi_i}\rangle\\&=\delta(\pi_i\pi,\pi_f)(2I_i+1)(2I_f+1)^{1/2}\sum_{\mu=-L}^{+L}(I_iLI_f\,|\,m_{q_1}+m_{q_2}-\mu\mu m_{q_1}+m_{q_2})\\&\quad\times\Bigg[\int_0^{\pi/2}d\beta\sin\beta\, d^{I_i}_{m_{q_1}+m_{q_2}-\mu;m_{q_1'}+m_{q_2'}}(\beta)t^{L\pi\mu}_{q_1q_2;q_1'q_2'}(\beta)\\&\qquad+\pi_i(-)^{I_i-(m_{q_1'}+m_{q_2'})}\int_0^{\pi/2}d\beta\sin\beta\, d^{I_i}_{m_{q_1}+m_{q_2}-\mu;-m_{q_1'}-m_{q_2'}}(\beta)\\&\qquad\times t^{L\pi\mu}_{q_1q_2;\bar{q}_1'\bar{q}_2'}(\beta)\Bigg],\end{aligned} \tag{16}$$

where

$$t^{L^\pi\mu}_{q_1q_2;q_1'q_2'}(\beta)\equiv\frac{1}{(2\pi)^2}\int_0^{2\pi}d\phi_p\int_0^{2\pi}d\phi_n e^{i(Z_0\phi_p+N_0\phi_n)}T^{L^\pi\mu}_{q_1q_2;q_1'q_2'}(\phi_p,\phi_n,\beta)$$
$$=\frac{1}{\pi^2}\int_0^{\pi}d\phi_p\int_0^{\pi}d\phi_n\left\{\mathrm{Re}\left[e^{i[Z_0(1/2)\phi_p+N_0(1/2)\phi_n]}T^{L^\pi\mu}_{q_1q_2;q_1'q_2'}(\tfrac{1}{2}\phi_p,\tfrac{1}{2}\phi_n,\beta)\right]\right.$$
$$\left.+\mathrm{Re}\left[e^{i[Z_0(1/2)\phi_p-N_0(1/2)\phi_n]}T^{L^\pi\mu}_{q_1q_2;q_1'q_2'}(\tfrac{1}{2}\phi_p,-\tfrac{1}{2}\phi_n,\beta)\right]\right\} \tag{17}$$

and

$$T^{L^\pi\mu}_{q_1q_2;q_1'q_2'}(\tfrac{1}{2}\phi_p,\tfrac{1}{2}\phi_n,\beta)\equiv\langle\{q\}_0\,|\,a_{q_2}(q)a_{q_1}(q)\hat{T}^{L^\pi}_\mu(\Delta Z_0,\Delta N_0)$$
$$\times\exp\{-i\beta\hat{I}_y-i\tfrac{1}{2}\phi_p\hat{Z}-i\tfrac{1}{2}\phi_n\hat{N}\}a^\dagger_{q_1'}(q')a^\dagger_{q_2'}(q')\,|\,\{q'\}_0\rangle\ . \tag{18}$$

Strictly speaking formula (17) holds only if $\hat{T}^{L^\pi}_\mu(\Delta Z_0,\Delta N_0)$ is a real operator. However, if $\hat{T}^{L^\pi}_\mu(\Delta Z_0,\Delta N_0)$ is complex it can always be split into a real and an imaginary part which can then be treated according to (17).

According to I the most general wave function constructable in the nonorthogonal configuration space (14),(15) is given by

$$|\{q\}i;Z_0N_0I^\pi M\rangle=|\{q\}_0;Z_0N_0I^\pi M\rangle f^{I^\pi}_{0;i}(q)+\sum_{\substack{q_1>0,q_2\\(|q_1|\le|q_2|)}}|\{q\}q_1q_2;Z_0N_0I^\pi M\rangle f^{I^\pi}_{q_1q_2;i}(q)\ , \tag{19}$$

where $|q_1|\le|q_2|$ refers to a suitable ordering of the quasiparticle states with $m_\alpha>0$. The configuration mixing degrees of freedom $f^{I^\pi}(q)$ are then obtained by the solution of the matrix equation

$$[H^{I^\pi}(q)-E^{I^\pi}(q)N^{I^\pi}(q)]f^{I^\pi}(q)=0 \tag{20}$$

under the constraint

$$[f^{I^\pi}(q)]^\dagger N^{I^\pi}(q)f^{I^\pi}(q)=U \tag{21}$$

which ensures the orthonormality of the states (19). U is here the unit matrix. $N^{I^\pi}(q)$ and $H^{I^\pi}(q)$ are the overlap and Hamiltonian matrix within the configuration space (14),(15). They can be easily calculated from the general expressions (16)—(18). The rotated matrix elements (18) for both the overlap as well as the Hamiltonian matrix have been given in Appendix B of I and will hence not be repeated here.

As in I here we would also like to stress that it is very essential to perform the number and spin projections before the diagonalization of the Hamiltonian (20),(21). Only such possible spin dependencies of the configuration mixing can be taken into account and, even more important, spurious admixtures due to the partial linear dependence of the intrinsic configurations (9) and (11) with respect to rotations can be avoided.[11]

The wave functions (19) contain up to 6qp correlations with respect to the already complicated HFB vacuum (9). This is due to the fact that the rotation operator applied on any of the configurations (9) or (11) yields a linear combination of all the $n$qp states (10) having the right number parity ($n=0$ up to $n=M_p+M_n$) while the Hamiltonian (2) contains at most four quasiparticle annihilation operators (see Appendix A of I). In the matrix element (18) of the Hamiltonian therefore (for $q=q'$) only up to 6qp configurations can contribute. Furthermore obviously not all the 4qp and 6qp configurations are included since the rotation operator creates only particular linear combinations. Nevertheless, since the projection is done before the variation, the system has at least some freedom to choose out of these 4qp and 6qp components those which are energetically most favored.

This admixture of 4qp and 6qp excitations is also the reason why in the wave functions (19) the projected 0qp states (14) do mix with the projected 2qp configurations (15). Thus, for example, a transition from the favored yrast configuration of the 0qp structure (14) to a 2qp structure (15) at certain spins as appears, for example, in some of the rare-earth nuclei (see, for example, Ref. 12) can be described here although a fixed mean HFB field is used for all the spin values. Obviously improvements could be reached by determining not only the configuration mixing but also the HFB transformation (3) itself after restoring the broken symmetries. Such even higher-order correlations with respect to the intrinsic structure of the 0^+ ground state could be accounted for. However, out of numerical reasons, this is not done in the present version of the MONSTER approach.

Lastly, the restriction to at most 6qp excitations with respect to the intrinsic vacuum (9) has the consequence that states with a more complicated structure cannot be described within the MONSTER approximation. Thus, for example, states with a predominant 8qp structure (in the limit of vanishing pairing these would be 4p4h states with respect to the corresponding Hartree-Fock vacuum) are cleary outside the MONSTER configuration space.

It is worthwhile to mention that the wave functions (19) account for K mixing in the intrinsic configuration space. Consequently the intrinsic structures corresponding to the laboratory wave functions (19) can have rather general de-

formations. Thus, for example, not only axially deformed nuclei but also nonaxial ones can be described within the present scheme.

Finally, we would like to point out that in the limit of vanishing pairing correlations the MONSTER wave functions (19) are identical to those of the projected particle-hole model on Hartree-Fock basis (PHM), which has been proposed a couple of years ago[13] and since been applied with some success to both the low excited as well as the giant multipole resonance states in some light doubly even self-conjugate nuclei.[11,14,15] The MONSTER can therefore be understood as a straightforward extension of the PHM approach accounting, unlike the latter, also for pairing correlations, which as we know are rather important at least as far as neutron excess nuclei are considered.

Unfortunately, in general the diagonalization (20),(21) of the effective Hamiltonian (2) in the configuration space (14),(15) is not yet sufficient to obtain reasonable wave functions (19). This is due to the fact that as soon as more than one major oscillator shell is included in the single-particle basis, the resulting many nucleon configurations usually contain admixtures due to center-of-mass excitations which have to be considered as spurious[16,17] and hence, at least approximately, to be eliminated. In the MONSTER approach this is achieved with the help of a method, which has been proposed by Giraud[17] and has also been applied in the PHM calculations[11,14,15] mentioned above. The procedure can be summarized as follows.

Instead of solving (20),(21) directly, the equivalent set of equations for the center of mass Hamiltonian $\hat{H}_{\text{c.m.}}$, which has a similar structure as the effective Hamiltonian (2), is solved first. If the configuration space (14),(15) would be complete with respect to center-of-mass excitations, most of the eigenvalues $e^{I^\pi}_{\text{c.m.}}(q)$ resulting from the solution of

$$[H^{I^\pi}_{\text{c.m.}}(q)-e^{I^\pi}_{\text{c.m.}}(q)N^{I^\pi}(q)]S^{I^\pi}(q)=0 \tag{22}$$

under the constraint

$$[S^{I^\pi}(q)]^\dagger N^{I^\pi}(q)S^{I^\pi}(q)=U \tag{23}$$

would be degenerate with the corresponding eigenstates of the form (19) describing the center of mass in its ground state. All the other solutions of (22),(23) [with eigenvalues $e^{I^\pi}_{\text{c.m.}}(q)$ being by $1\hbar\omega, 2\hbar\omega, \ldots$, larger than the ground-state value] are then the spurious center-of-mass excitations $|s\rangle$ $(s=1,\ldots,n_s)$. With the use of the projection operator

$$\hat{P}_s \equiv 1-\sum_{s=1}^{n_s} |s\rangle\langle s| \tag{24}$$

to modify the original Hamiltonian (2) into

$$\hat{\tilde{H}} \equiv \hat{P}_s \hat{H} \hat{P}_s \tag{25}$$

and solving the problem

$$[\tilde{H}^{I^\pi}(q)-E^{I^\pi}(q)N^{I^\pi}(q)]f^{I^\pi}(q)=0 \tag{26}$$

with

$$[f^{I^\pi}(q)]^\dagger N^{I^\pi}(q)f^{I^\pi}(q)=U \tag{27}$$

instead of (20),(21), then yields the n_s spurious states at energy $E^{I^\pi}(q)\equiv 0$ while all the other solutions are free from admixtures due to the center-of-mass motion. Obviously in practical calculations the configuration space will usually not be complete with respect to $\hat{H}_{\text{c.m.}}$. However, even then the eigenvalues $e^{I^\pi}_{\text{c.m.}}(q)$ will still be clustered around the exact values.[11,15,17] At least the predominantly spurious states can therefore still be eliminated using the above procedure, which is very essential especially if low excited negative parity states are to be considered.

With the use of the obtained MONSTER wave functions (19) now with the help of the general expressions (16)—(18) all the physical quantities, which may be of interest for the particular problem under consideration, for example, electromagnetic moments and transitions as well as the corresponding transition densities can be calculated. This is one of the main advantages of the MONSTER method with respect to, for example, the self-consistent HFB cranking approach,[18–20] which up to now has been the only microscopic model available for the description of high-spin states in the rare-earth region. Though simulating an approximate projection before the variation of the mean-field parameters, which is not done in the MONSTER approximation, the HFB cranking approach does not produce quantum-mechanical many body wave functions with the required symmetry properties. Instead the cranking wave functions usually contain large angular momentum fluctuations,[21] which, especially in band crossing regions, lead to serious complications. Improvements can be reached if higher-order terms are introduced.[22] However, this helps only for expectation values like the energy or magnetic moments. Transitions between states, on the other hand, can hardly be obtained within the cranking approach.

III. THE NUMERICAL PROCEDURE

During the last three years a computer code has been developed, which allows the application of the MONSTER approach discussed in the last section to a huge amount of nuclear structure problems in various mass regions. This code was designed for the 1100/80 Univac computer at the University of Tübingen. The same version has also been installed on the IBM facilities at the Kernforschungsanlage Jülich. In the present paper we shall not describe this code in detail. Instead we shall briefly summarize how in practice a MONSTER calculation is done and discuss the possibilities and limitations along the way.

First, a single particle basis is chosen. In its present version the code can handle systems like $0s$-$2s\,1d\,0g$ for light nuclei or the Kumar-Baranger basis[23] ($N=4,5$ for protons, $N=5,6$ for neutrons). Larger basis spaces cannot be used on the Tübingen Univac out of storage reasons. On larger computers, however, like the Jülich IBM, an extension to larger basis systems is straightforward.

Second, an effective Hamiltonian for this basis system is chosen. Here any arbitrary interaction, which can be

represented by coupled two-body matrix elements, can be taken. Furthermore, it is possible to use different sets of coupled two-body matrix elements for proton-proton, neutron-neutron, and proton-neutron interactions. Besides the restriction to two-body forces no further approximation is needed. The one-body term may also be arbitrarily chosen.

Third, the two-body matrix elements are decoupled and suitably stored for later use.

Fourth, a standard HFB calculation is performed for the nucleus under consideration. Here the numerical method proposed by Mang *et al.*[24] is used. Initial values for the iteration are provided by a Nilsson plus BCS calculation. Restrictions here are the neglect of parity mixing and of the proton-neutron pairing as well as the requirement of axial symmetry for the quasiparticle transformation (3).

Fifth, the chosen effective Hamiltonian (2), the center-of-mass Hamiltonian $\hat{H}_{\text{c.m.}}$, and the number operators $\hat{Z}$ and $\hat{N}$ are transformed into the quasiparticle representation (see Appendix A of I) and suitably stored.

Sixth, all the spin- and number-rotated matrices of Appendix B of I, except the interaction term, are calculated. For this purpose suitable points for the later integration have to be chosen. For the angular momentum projection usually a Gaussian integration with up to 20 points from 0 to $\pi/2$ is performed. This limits the validity of the results to about spin $I=26$. An extension to larger spins would require an increase of the number of angles to be used. Such an extension is easily possible; however, it increases the computer time linearly. For the number projection the integral operators (12) are discretized. Instead of the integrals in Eq. (17) one uses the sums

$$t^{L^\pi\mu}_{q_1,q_2;q_1'q_2'}(\beta)\equiv\frac{1}{L_pL_n}\sum_{k_p=0}^{L_p-1}\sum_{k_n=0}^{L_n-1}\left[\mathrm{Re}\left\{\exp\left[i\left[N_0\frac{\pi}{4L_n}(2k_n+1)+Z_0\frac{\pi}{4L_p}(2k_p+1)\right]\right]\right.\right.$$
$$\left.\times T^{L^\pi\mu}_{q_1q_2;q_1'q_2'}\left[\frac{\pi}{4L_p}(2k_p+1),\frac{\pi}{4L_n}(2k_n+1),\beta\right]\right\}$$
$$+\mathrm{Re}\left\{\exp\left[i\left[Z_0\frac{\pi}{4L_p}(2k_p+1)-N_0\frac{\pi}{4L_n}(2k_n+1)\right]\right]\right.$$
$$\left.\left.\times\ T^{L^\pi\mu}_{q_1q_2;q_1'q_2'}\left[\frac{\pi}{4L_p}(2k_p+1),-\frac{\pi}{4L_n}(2k_n+1),\beta\right]\right\}\right] \tag{28}$$

which hold for L_p,L_n both larger than or equal to 1. It is easy to show that besides the desired particle numbers Z_0,N_0, (28) contains only admixtures from $Z_0\pm4L_p\nu$ ($\nu=1,2,\ldots$) and $N_0\pm4L_n\nu$ ($\nu=1,2,\ldots$). In practical calculations usually $L_p=L_n=3$ is sufficient. The quality of this approximation is checked by calculating the particle number expectation values in the final wave functions (19). In principle, the code could handle $L_p=L_n\leq16$. However, this leads to a drastic (more than linear) increase in the computer time.

Seventh, a configuration space is chosen. Here either all 2qp configurations, or only those up to a certain K value, or only those up to a certain unperturbed intrinsic excitation energy, or a particular number of arbitrarily chosen ones can be used. After calculating the interaction terms then the matrices (18) of the Hamiltonian, the overlap, the center-of-mass Hamiltonian, and the number operators are set up and number projected according to Eq. (28). Here separate steps are used for the positive and the negative parity states. Because of storage restrictions on the Univac the present MONSTER version can only handle up to 440 2qp configurations in these steps. On larger machines an extension is easily possible.

Eighth, the number projected matrices (28) are spin projected according to Eq. (16).

Ninth, alternately to steps 7 and 8, the corresponding number and spin projected matrices within the 1qp states to be constructed from (9) can also be calculated. This allows an approximate description of the low-energy spectra of the odd-A nuclei around the considered doubly even nucleus, similarly as has been done in Ref. 4. Here all the 1qp states are always taken into account.

Tenth, the matrix equations (22),(23) and (26),(27) are solved. This is done using standard methods discussed by Wilkinson.[25] The resulting energies and wave functions are stored. Due to the storage shortage on the Univac in this step of the program only up to 235×235 matrices can be handled. On a larger computer, however, this number can be easily increased.

Eleventh, electromagnetic transitions of arbitrary L^π can be calculated. Each multipolarity requires a different run. The procedure is similar to the energy calculation: First, the rotated matrices are calculated, then the number and spin projections performed, and finally the transition amplitudes in between the wave functions (19) calculated.

Twelfth, for particular states the electromagnetic transitions may be analyzed in terms of spectroscopic amplitudes $[C_i^\dagger C_j]^{L^\pi}_\mu$ for the spherical basis states. Thus, for example, occupation numbers or general transition densities may be obtained. The latter may then for example be

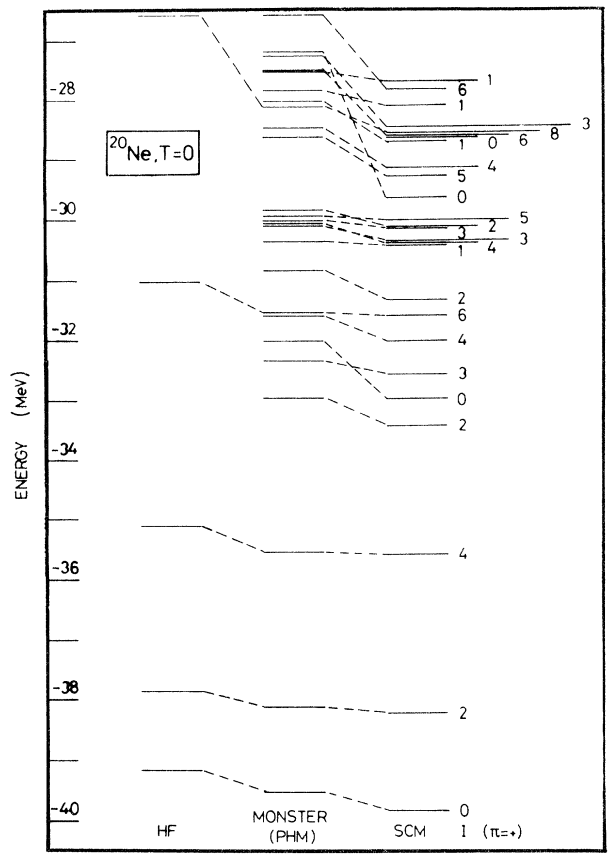

FIG. 1. Lowest isoscalar ($T=0$) states for the nucleus ^{20}Ne as obtained in an $1s\,0d$ basis using single-particle energies and a MSDI from the literature (Ref. 26) as effective Hamiltonian. In this case we obtain no pairing. Therefore the HFB solution (14) is identical to the HF approach and the MONSTER reduces to the PHM approximation (Refs. 11 and 14). Both spectra are compared to the results of a complete shell model diagonalization (SCM).

used as input for distorted-wave Born approximation (DWBA) calculations in order to analyze inelastic proton scattering or similar processes.[15] This step of the code is by far the most time consuming.

Actual computer times for MONSTER calculations will be given at the end of the next section.

IV. RESULTS AND DISCUSSION

In order to check the quality of the MONSTER approximations discussed in Sec. II of the present paper we have first studied some problems for which complete shell model diagonalizations[26,27] (SCM) are numerically still possible. As examples for such problems we shall discuss here calculations for the two nuclei ^{20}Ne and ^{22}Ne using only the $1s\,0d$-oscillator orbits as single-particle basis and choosing spherical single particle energies plus the modified surface delta interaction[28] (MSDI)

$$V_{\mathrm{MSDI}}(1,2)=-4\pi A_T\delta(\Omega_{12})\delta(r_1-R)\delta(r_2-R)+B_T \tag{29}$$

as effective Hamiltonian (2). The parameters of this interaction ($A_0=0.77$ MeV, $A_1=0.95$ MeV, $B_0=-2.51$ MeV, and $B_1=0.37$ MeV) as well as the single-particle energies [$\epsilon(d_{5/2})=-4.49$ MeV, $\epsilon(s_{1/2})=-3.16$ MeV, and $\epsilon(d_{3/2})=1.05$ MeV] have been taken from the literature.[26] The SCM calculations have been performed[29] partly with the Glasgow[27] and partly with the Oak Ridge–Rochester[26] shell model computer codes.

For ^{20}Ne the standard HFB procedure yields an unpaired intrinsic prolate solution which coincides with the Hartree-Fock (HF) solution already discussed in Ref. 14. Angular momentum projection of the HF reference determinant leads then to the yrast spectrum labeled by HF on the left side of Fig. 1. Because of the lack of pairing the intrinsic 2qp configurations (11) are then all one-particle–one-hole (1p1h) excitations with respect to the HF vacuum. Using all these 1p1h configurations (altogether 20 in the considered example) plus the HF vacuum as configuration space for the MONSTER calculation one obtains the states labeled by MONSTER (PHM) displayed in the middle of Fig. 1. This is exactly the same spectrum as obtained using the PHM approach in Ref. 14. Finally, on the right side of Fig. 1, the results of the complete shell model diagonalization (SCM) are given. As for the MONSTER spectrum also here for simplicity only the lowest isoscalar ($T=0$) states have been plotted.

It is evident from the figure that the inclusion of correlations via the projected 1p1h configurations yields a considerable improvement for the ^{20}Ne yrast levels. So, for example the 0^+ ground state is lowered by almost 400 keV and the energy gain for the 8^+ level even exceeds 1500 keV. The resulting MONSTER-(PHM) spectrum is in rather good agreement with the exact shell model results. This holds not only for the yrast levels but also for most of the excited states except the three 0^+ excitations and the bands being based on them. However, these states are known[30] to be of predominant 4p4h structure with respect to the deformed HF vacuum and hence cannot be expect-

TABLE I. Selected $B(E2)$ values for ^{20}Ne as obtained by either the MONSTER (here identical to the PHM) or the SCM calculations. In both cases effective charges of $1.5e$ for protons and $0.5e$ for neutrons have been used.

$I_i^{\pi_i}/\hbar$	$I_f^{\pi_f}/\hbar$	MONSTER-$B(E2)/e^2\mathrm{fm}^4$	SCM-$B(E2)/e^2\mathrm{fm}^4$
0_1^+	2_1^+	289.1	282.1
	2_2^+	0.1	0.2
	2_3^+	1.4	0.8
2_1^+	4_1^+	120.9	119.2
	2_2^+	4.2	6.0
	0_2^+	1.3	2.5
	3_1^+	0.2	0.1
	4_2^+	8.2	8.7
	2_3^+	0.1	0.0
4_1^+	2_2^+	0.1	0.0
	3_1^+	5.6	5.8
	4_2^+	4.9	5.4
	6_1^+	75.0	72.7
	2_3^+	1.0	1.4
6_1^+	8_1^+	40.2	34.8

ed to be reproduced within the MONSTER configuration space, which as has been discussed in Sec. II takes into account only up to 6qp correlations (i.e., 3p3h configurations in the limit of vanishing pairing).

The good agreement with the SCM results is not restricted to the excitation energies but holds also for quantities being much more sensitive to details of the nuclear wave functions than the latter. As an example we compare in Table I a couple of selected $B(E2)$ values as obtained with either the MONSTER or the SCM approach. In both calculations effective charges of $1.5e$ for the protons and $0.5e$ for the neutrons have been used. Again the agreement of the approximate MONSTER with the exact SCM results is rather striking.

Let us now turn our attention to the nucleus ^{22}Ne. Here an intrinsic prolate HFB solution is obtained which is again unpaired as far as the protons are considered, but now contains correlations from neutron-neutron pairing. Consequently now the projected HF-yrast band displayed in the first column of Fig. 2 differs from the HFB ground band (14) shown in the second column. Owing to the neutron pairing correlations energy gains of about 750, 450, and 100 keV are obtained for the 0^+, 2^+, and 4^+ members of the yrast band and such, as expected, the effective moment of inertia is decreased. Owing to the breakdown of the pairing correlations with increasing spin, however, at higher spin values the projected HF states are expected to be energetically favored. This is clearly seen for the 6^+ and 8^+ members of the ground band.

Using the intrinsic HF solution as reference and including all the possible 1p1h excitations with respect to it (altogether 26) in the configuration space one obtains now the PHM spectrum shown in the third column of Fig. 2 while the MONSTER calculation being based on the HFB reference determinant and including all the 46 possible 2qp configurations yields the spectrum displayed in column four. Finally, in the last column of Fig. 2, the results of the complete SCM calculation are given. Again the agreement between the MONSTER and the SCM results is surprisingly good especially if the MONSTER ground-state energy being about 300 keV above the SCM result is renormalized to the latter and only relative excitation energies are compared. Again the excited 0^+ states are the levels which are worst reproduced by the MONSTER approach though here in ^{22}Ne due to the partial blocking of 4p4h excitations by the two extra neutrons the agreement is even somewhat better than in the ^{20}Ne case discussed above. It is furthermore interesting to note that as far as the higher spin states are considered, the PHM results are not far away from those of the MONSTER calculation. For the lower spin states, however, especially the 0^+ and 2^+ levels, the MONSTER approach is obviously far superior such showing the importance of pairing correlations even in light deformed neutron excess nuclei.

In Table II selected $B(E2)$ values are obtained with the PHM, the MONSTER, and the SCM approach for the nucleus ^{22}Ne. Again an effective extra charge of 0.5e for both protons and neutrons has been used in all the calculations. As in ^{20}Ne also here the MONSTER reproduces the exact SCM results with a rather satisfying accuracy.

The results discussed so far show that, except for those

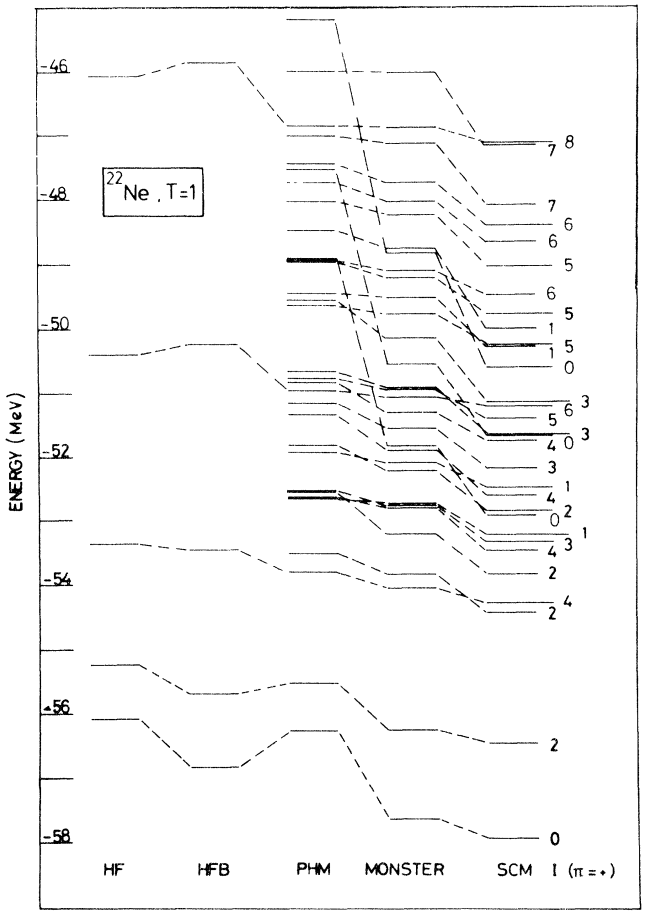

FIG. 2. Lowest $T=1$ states for the nucleus ^{22}Ne obtained with the same basis and effective Hamiltonian as the ^{20}Ne results in Fig. 1. Here neutron pairing does contribute. Therefore the HFB result (14) differs from the HF approach and also the MONSTER is not identical to the PHM limit. Again the results are compared with those obtained by a complete shell model diagonalization (SCM).

states which because of their predominant 8qp or even more complicated structure are not accounted for in our configuration space, the MONSTER approximations seem to be indeed rather well justified. This gives us some confidence that the MONSTER may be considered as a reasonable approximation to the exact SCM wave functions also in such model spaces, in which the latter are numerically unaccessible.

As a first step in this direction we have considered the nucleus ^{46}Ti in a single-particle basis including all the $1p0f$ orbits. As an effective two-body interaction here the matrix elements of Kuo and Brown[31] with the modifications introduced by McGrory[32] have been used. The single-particle energies have been taken from Ref. 33. The intrinsic HFB calculation for ^{46}Ti using the defined effective Hamiltonian (2) yields a prolate reference determinant which is paired not only on the neutron but also on the proton side. In the chosen single-particle basis therefore altogether 200 2qp configurations of the type (11) exist. However, many of those correspond to the creation of ei-

TABLE II. Selected $B(E2)$ values for ^{22}Ne. The results of the PHM, the MONSTER, and the SCM calculations are compared. The same effective charges as in ^{20}Ne have been taken.

$I_i^{\pi_i}/\hbar$	$I_f^{\pi_f}/\hbar$	$B(E2)/e^2\,\mathrm{fm}^4$ PHM	MONSTER	SCM
0_1^+	2_1^+	283.4	287.0	279.1
	2_2^+	5.1	3.3	4.9
	2_3^+	22.4	19.3	16.3
2_1^+	2_2^+	0.6	7.9	6.8
	4_1^+	139.2	128.7	124.5
	2_3^+	0.9	0.9	1.2
	4_2^+	0.4	1.1	4.1
	3_1^+	2.3	1.0	1.5
2_2^+	4_1^+	7.2	0.4	1.4
	2_3^+	0.3	3.6	11.7
	4_2^+	47.3	10.0	11.9
	3_1^+	143.3	130.1	97.0
4_1^+	2_3^+	0.8	5.6	3.7
	6_1^+	103.9	100.1	95.3
6_1^+	8_1^+	56.1	56.5	44.4
8_1^+	10_1^+	15.1	14.9	8.7

ther two particles in completely empty orbits or of two holes in completely occupied orbits and hence do not contribute to the wave functions for the nucleus under consideration. We have therefore included in our calculations only those 2qp excitations (11), for which $u_{q_1}v_{q_2}+v_{q_1}u_{q_2}$ is larger or equal to 0.09 where $v_{q_i}^2$ $(i=1,2)$ is the occupation number of the orbit q_i and $u_{q_i}^2=1-v_{q_i}^2$. Doing so the configuration space consists finally only of 139 2qp configurations besides the reference determinant (9). Of those 79 are neutron excitations while in 60 configurations the two quasiparticles are in proton orbits.

Since to our knowledge there exists no complete SCM calculation for ^{46}Ti using the full $1p0f$ shell as single-particle basis, unfortunately here the MONSTER results can only be compared to those of other approximate calculations. Several such results can be found in the literature. So, for example, Kutschera, Brown, and Ogawa[34] calculated the ^{47}Ti spectrum within the $(f_{7/2})^n$ model using the so-called ^{42}Sc interaction the matrix elements of which have been phenomenologically derived from the ^{42}Sc spectrum. Their results will be referred to as KBO in the following. Furthermore, a calculation using exactly the same single-particle basis and effective Hamiltonian as we do has been published by Müther *et al.*[33] They used a generator coordinate superposition of HFB solutions corresponding to different intrinsic quadrupole deformations and on top of these solutions a couple of time reversal invariant $K=0$ 2qp states to describe the ^{46}Ti wave functions. This calculation will be referred to as GCM + QP below. Another calculation for the ^{46}Ti has been performed by Skouras[35] who used a kind of angular-momentum-projected many determinant approach allowing even for particular 2p2h excitations of the ^{40}Ca core. These results will be labelled by SK in the following. Finally we shall compare the MONSTER results with the projected HFB spectrum (14) referred to as HFB and, lastly, with the experimental data (EXPT).[36–41]

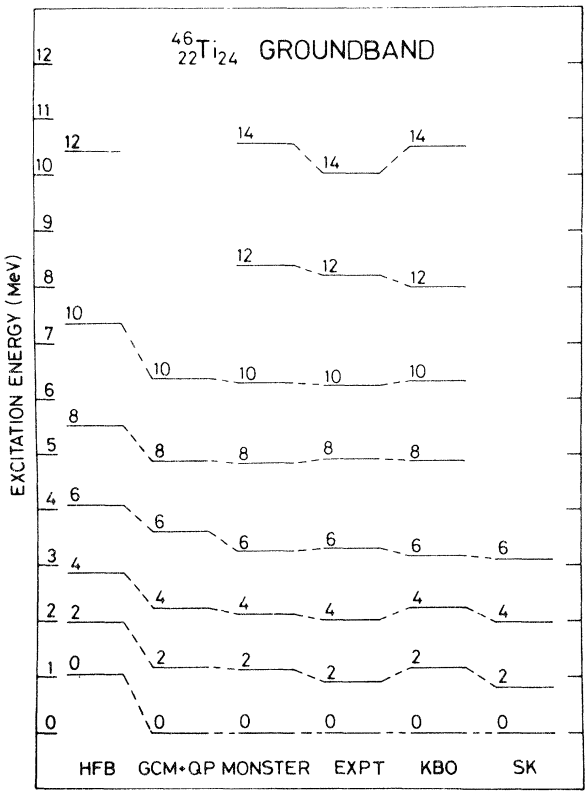

FIG. 3. ^{46}Ti ground bands as obtained by various methods are compared to the experimental data (Ref. 40). The HFB, the GCM + QP (Ref. 33), and the MONSTER results have been obtained using a full $1p0f$ basis and as effective Hamiltonian the matrix elements by Kuo (Ref. 31) with the modifications of McGrory (Ref. 32). On an absolute scale the GCM + QP ground state would be about 500 keV above the MONSTER result (Ref. 42). KBO refers to the $(f_{7/2})^n$ model with the ^{42}Sc interaction (Ref. 34) and SK to the calculation by Skouras (Ref. 35) which includes particular excitations of the ^{40}Ca core.

TABLE III. Spectroscopic quadrupole moments $Q(I)$ and g factors $g(I)$ for the yrast and some selected nonyrast states in ^{46}Ti. In the $(f_{7/2})^n$ model with the ^{42}Sc interaction (KBO) (Ref. 34) an effective extra charge of $0.9e$ for both protons and neutrons has been used. In the present calculation (MONSTER) this value was reduced to $0.7e$. For the calculation of the g factors in both calculations the bare single nucleon g factors have been used. The rotational limit for the $g(I)$ is $g_R = Z/A = 0.48$. Experimentally only the quadrupole moment of the first 2^+ state is known (Ref. 41): $Q(2_1^+) = -28 \pm 14$ e fm^2.

	$g(I)/\mu_N$		$Q(I)/e$ fm^2	
$I_i^\pi/\hbar$	KBO	MONSTER	KBO	MONSTER
2_1^+	0.52	0.34	13.19	−16.53
4_1^+	0.09	0.35	11.44	−25.13
6_1^+	0.34	0.63	−2.16	−25.69
8_1^+	0.25	0.60	3.42	−29.24
10_1^+	0.63	0.61	−25.63	−35.59
12_1^+	0.53	0.48	−22.48	−27.65
14_1^+	0.40	0.40	−23.63	−30.67
16_1^+		−0.38		−25.31
2_2^+	0.31	0.84	−1.35	10.54
4_2^+	−0.41	0.02	−16.75	0.83
6_2^+	0.82	0.21	−17.37	−8.63
8_2^+	0.68	0.14	−15.72	−10.80
7_1^+	0.18	0.41	1.29	−11.14
9_1^+	0.62	0.41	−12.53	−16.35
11_1^+	0.53	0.48	−21.85	−26.98

Figure 3 shows the ground bands of ^{46}Ti as obtained with these different methods and compares them to the experimental data.[40] Since most of the theoretical results have been obtained using different Hamiltonians, unfortunately only the relative energies can be compared. Therefore, all the spectra except for the HFB result which has been plotted at its proper energy relative to the MONSTER spectrum have been renormalized to the experimental ground-state energy. The GCM + QP band, which was obtained with exactly the same Hamiltonian as the MONSTER spectrum, yields an absolute 0^+ energy being about 500 keV less bound than the MONSTER ground state.[42]

Comparing the relative excitation energies in the

TABLE IV. Selected $B(E2)$ transitions in ^{46}Ti. In the $(f_{7/2})^n$ model with the ^{42}Sc interaction (KBO) (Ref. 34) an effective extra charge of $0.9e$ for both protons and neutrons has been used. In the present calculation (MONSTER) this value was reduced to $0.7e$. The experimental values are from Refs. 36–40.

		$B(E2; I_i^\pi \to I_f^\pi)/e^2$ fm^4		
$I_i^\pi/\hbar$	$I_f^\pi/\hbar$	(KBO)	MONSTER	EXPT
2_1^+	0_1^+	116	138	215±20
4_1^+	2_1^+	128	186	206±39
6_1^+	4_1^+	110	189	147±29
8_1^+	6_1^+	123	172	108±20
10_1^+	8_1^+	69	119	118±29
12_1^+	10_1^+	42	51	29±3
14_1^+	12_1^+	29	49	49±20
16_1^+	14_1^+		0	
2_2^+	0_1^+	2	4	2
2_2^+	2_1^+	38	92	157
12_1^+	11_1^+	25	22	
11_1^+	10_1^+	5	7	< 157
8_2^+	8_1^+	33	9	$< 50[9^+ \to 8_1^+]$
	6_1^+	0	0	
	6_2^+	49	93	
6_2^+	4_1^+	4	0	
	6_1^+	55	18	
5_2^+	6_1^+	0	1	
	6_2^+	1	33	
	4_1^+	13	6	

ground band with the experimental data one has to conclude that all the calculations do rather well. So, for example, the average deviation from the experimental excitation energies up to the 10^+ yrast state are only 110 (MONSTER), 150 (KBO), 190 (GCM + QP), and 210 (HFB) keV (Skouras gives only results for $I^\pi \leq 6^+$) and even if the recently measured[40] 12^+ and 14^+ states are included the average deviations of the MONSTER and KBO energies being 180 and 200 keV, respectively, are still rather small. On the other hand, the HFB spectrum cannot reproduce these high spin states and yields now an average deviation of about 600 keV.

Far worse is the agreement between the different methods if the excited states are considered, selected ones of which are displayed in Fig. 4. Here the MONSTER reproduces the experimental data[38–40] much better than the other methods. The GCM + QP method, which by the way yields only even spin states since it was restricted to time reversal invariant configurations, yields systematically higher, and the KBO approach systematically lower excitation energies than the MONSTER. This becomes especially evident if one considers, for example, the lowest $I=5^+$, 7^+, and 11^+ states as well as the lowest nonyrast 2^+ and 6^+ levels. On the other hand, the lowest excited 0^+ state is only reproduced by Skouras's calculation. This state seems to be of predominant 8p2h structure with respect to the ^{40}Ca core and lies therefore outside the MONSTER model space which was restricted to the $1p0f$ orbits.

Further support for the MONSTER approach especially with respect to the KBO model comes from the g factors $g(I)$ and the spectroscopic quadrupole moments $Q(I)$ displayed in Table III as well as from the $B(E2)$ values given in Table IV. So, for example, the KBO calculation yields an oblate shape for the 2^+ member of the yrast band [$Q(2^+)=13$ $e\,\mathrm{fm}^2$], while the MONSTER giving $Q(2^+)=-17$ $e\,\mathrm{fm}^2$ reproduces the experimentally established prolate deformation of $Q(2^+)=-28\pm14$ $e\,\mathrm{fm}^2$ (Ref. 41) rather nicely. Drastic discrepancies between the KBO method and the MONSTER approach are also obtained for the spectroscopic quadrupole moments and g factors of the other yrast and nonyrast states listed in Table III for which, unfortunately, no experimental data are available. Especially in the yrast band the small model space used in the $(f_{7/2})^n$ model leads to strongly varying $g(I)$ and $Q(I)$ values while the MONSTER approach yields a more stable structure for these states. The advan-

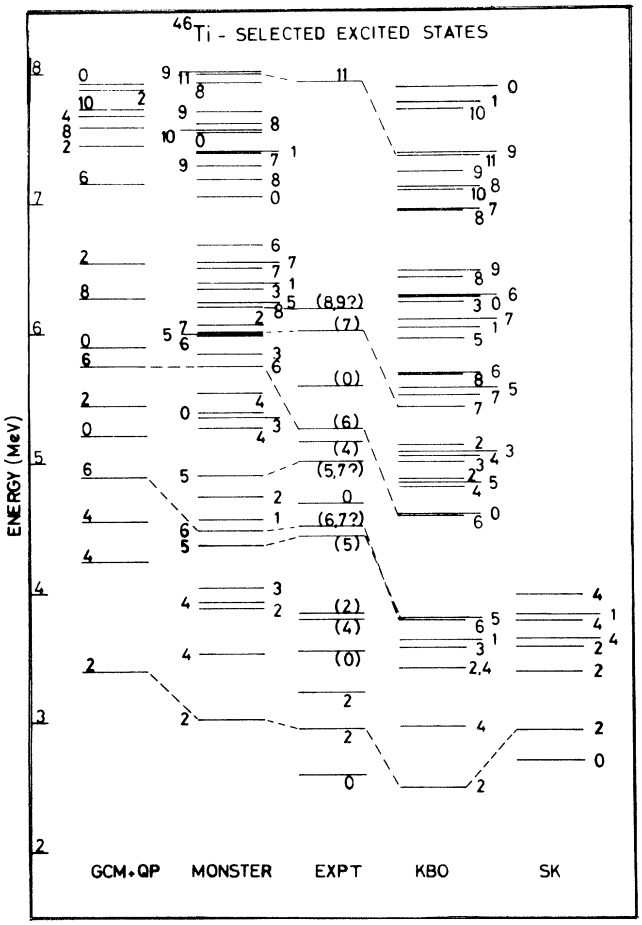

FIG. 4. Selected excited states for ^{46}Ti. Methods and forces are the same as in Fig. 3. Note that the GCM + QP approach (Ref. 33) yields only even spin values since it was restricted to time-reversal invariant $K=0$ configurations.

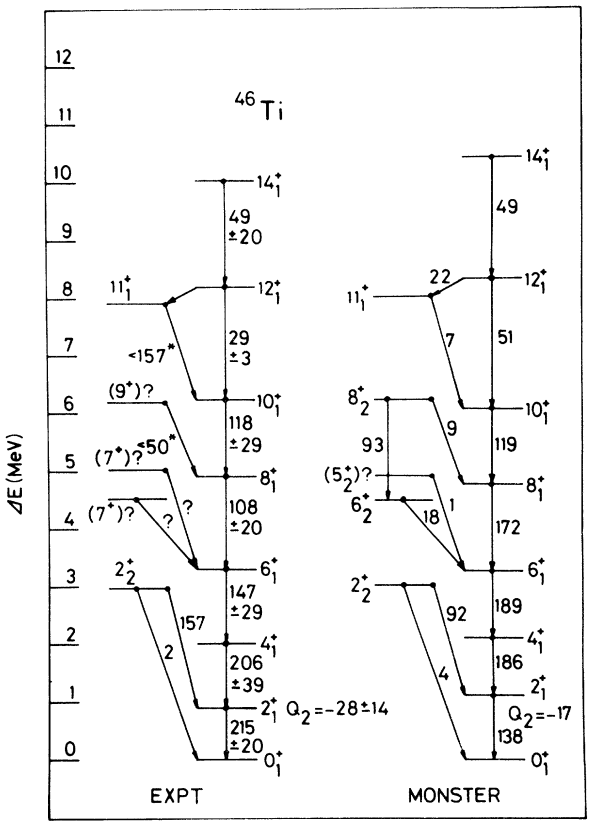

FIG. 5. Ground band and selected excited states of ^{46}Ti as obtained by the MONSTER are compared to the experimental data (Ref. 40). In addition to the energies here also the $B(E2)$ values are given. Their units are $e^2\,\mathrm{fm}^4$. Furthermore also the spectroscopic quadrupole moment Q_2 of the lowest 2^+ state is given. The experimental data have been taken from Refs. 36–41. An asterisk indicates that a pure $E2$ decay has been assumed.

tage of the larger model space is also reflected in the appearance of an $I^{\pi}=16^{+}$ state (about 150 keV above the 14^{+} yrast level) while the maximum spin possible in the KBO basis system is $I^{\pi}=14^{+}$. Unfortunately, this 16^{+} level has only extremely small γ-transition probabilities to any of the lower excited states and therefore decays most probably by particle emission. Hence it could not be observed in the recent experiments establishing the ground band up to the 14^{+} level.[40]

The superiority of the MONSTER approach is also evident from the $B(E2)$ values listed in Table IV. Here the MONSTER also reproduces the experimental data[36–41] much better than the KBO method. Using different effective charges for the various single-particle matrix elements of the $E2$ operator, as should in principle be done,[43] obviously even further improvements should be reached here.

Finally, in Fig. 5, we compare the MONSTER predictions for the yrast and a few nonyrast states with the experimental level scheme proposed in Ref. 40. In addition to the excitation energies here also the $B(E2)$ values (in units of $e^2\,\mathrm{fm}^4$) and the spectroscopic quadrupole moment of the lowest 2^{+} state (in units of $e\,\mathrm{fm}^2$) are displayed. As can be easily seen the overall agreement of the two level schemes is rather striking. The only open problems are obviously the three side states at 4524, 5024, and 6201 keV for which no clear spin assignment but only some suggestions have been given in Ref. 40. For the 6201-keV level the authors of Ref. 40 suggested a spin value of $I^{\pi}=9^{+}$ essentially because no γ transition from this state to the 6^{+} yrast level was observed and furthermore since the KBO calculation predicts a 9^{+} level at about 6.5 MeV (see Fig. 4). In the MONSTER calculation, however, no 9^{+} state below 7.2 MeV excitation energy is obtained. Instead the only level in the right energy region which shows a considerable transition probability to the 8^{+} yrast level and which has the experimentally observed property not to decay to the 6^{+} member of the yrast band is the second 8^{+} state (see also Table IV). Thus we would propose spin 8^{+} for the 6201-keV level. Similar arguments hold for the 4524-keV level. Here our candidate would be the second 6^{+} state, which like the corresponding experimental level does also not decay to the 4^{+} yrast state (see also Table IV). For the middle state at 5024 keV, however, we have a problem. Here the most suitable theoretical candidate would be the second 5^{+} level. Unfortunately, as can be seen from Table IV, this state does decay to the 4^{+} yrast level in contradiction to the experimental findings. Therefore, this state is given with a big question mark in Fig. 5. Another open question is definitely why the large $B(E2)$ value obtained theoretically between the second 8^{+} and 6^{+} states is not observed experimentally. Thus also our suggestions for the three side levels have to be considered only as preliminary and some more experimental data and perhaps also theoretical calculations are needed before the assignment problem for these three side levels can be solved satisfactorily. Nevertheless, we may conclude that for the ^{46}Ti case the MONSTER works rather well. It may therefore be worthwhile to study also some neighboring nuclei with this method. Such calculations are in preparation.

As the last test to be discussed in the present paper, we have applied the MONSTER to the nucleus ^{164}Er. For this calculation a single-particle basis consisting of the $N=4$ plus the $0h_{11/2}$ and $0h_{9/2}$ oscillator orbits for the protons and out of the $N=5$ plus the $0i_{13/2}$ and $1g_{9/2}$ states for the neutrons has been used. The same basis system has been widely in use by the Munich group.[18,24] As single-particle energies those of Baranger[23] and Kumar have been taken and the effective interaction was an *ad hoc* chosen pairing plus quadrupole pairing plus quadrupole-quadrupole force with monopole and quadrupole pairing strengths of $G_p(I=0)=G_p(I=2)=31/A$ MeV for the proton-proton and of $G_n(I=0)=G_n(I=2)=24/A$ MeV for the neutron-neutron matrix element and with quadrupole-quadrupole strength parameters of $\chi'_{pp}=\chi'_{nn}=73A^{-1.4}$ MeV and $\chi'_{pn}=100A^{-1.4}$ MeV. Obviously all the exchange terms of this interaction are accounted for in the calculations. Furthermore in the calculations a constant effective moment of inertia for the case of $\theta_c/\hbar^2=5.8\ \mathrm{MeV}^{-1}$ has been introduced, and as configuration space only the 65 determinants (9),(11) with the lowest unperturbed intrinsic excitation energies have been taken.

Figure 6 shows the obtained yrast and yrare bands and

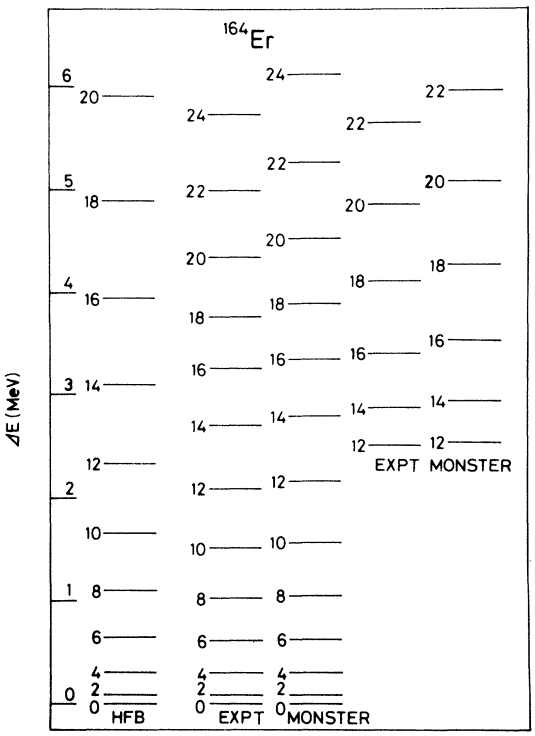

FIG. 6. MONSTER results for the ground and the s band of ^{164}Er are compared to the experimental data (EXPT) (Refs. 44 and 45). In addition the HFB spectrum (14) is displayed. As single-particle basis for the protons the $N=4$ shell plus the $0h_{11/2}$ and $0h_{9/2}$ orbits and for the neutrons the $N=5$ shell plus the $0i_{13/2}$ and $1g_{9/2}$ orbits have been used. The single-particle energies have been taken from Kumar and Baranger (Ref. 23) and as effective interaction a pairing plus quadrupole pairing plus quadrupole-quadrupole force was used. The parameters of this force are given in the text. Furthermore a constant moment of inertia of the core $\theta_c/\hbar^2=5.8\ \mathrm{MeV}^{-1}$ has been introduced.

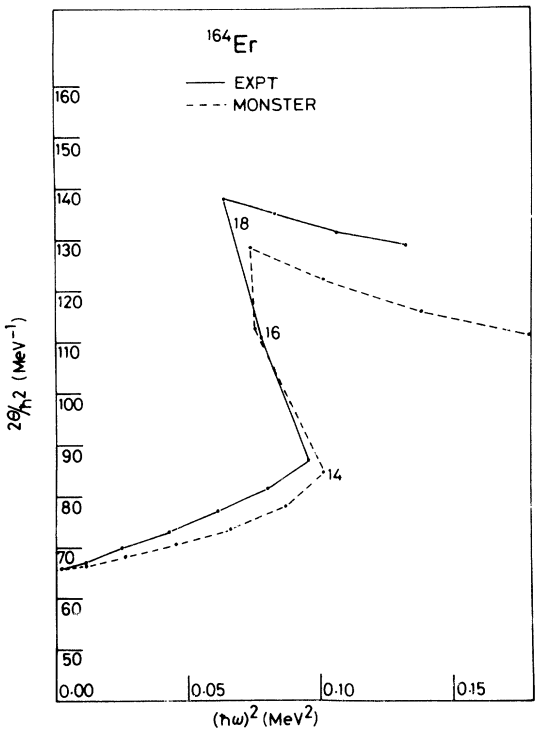

FIG. 7. Backbending plot for the yrast band displayed in Fig. 6. For the calculation of the rotational frequency $\hbar\omega$ and the effective moment of inertia $\theta/\hbar^2$ the convention of Ref. 12 has been used. The experimental data are again from Ref. 45.

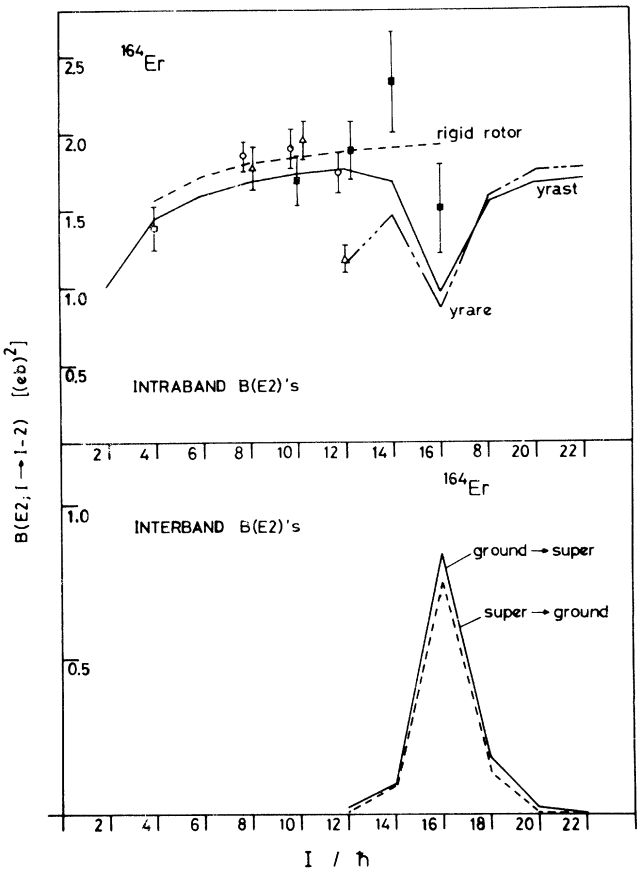

FIG. 8. Quadrupole transition probabilities $B(E2;I\rightarrow I-2)$ inside and in between the yrast and the yrare bands of ^{164}Er are displayed. For the MONSTER calculation the Kumar-Baranger (Ref. 23) effective charges of $e_p=1.622e$ and $e_n=0.622e$ have been used. The experimental data have been taken from the compilation in Ref. 45. Open squares refer to lifetime measurements by a microwave technique (Ref. 46), open triangles to the Doppler-broadened line-shape measurements of Ref. 47. The open circles label also Doppler-broadened line-shape measurements but now from Ref. 45 and the black squares have been extracted from multiple Coulomb excitation measurements (Ref. 45). For comparison also the rigid rotor prediction (dashed line in the upper half of the figure) is given. More detailed information about the MONSTER results may be found in Tables IV and V.

compares them with the HFB result (14) as well as with the experimental data.[44,45] It is clearly seen that while the HFB result starts to deviate from the experimental spectrum already at low spins, the MONSTER yields a rather good description of the experimental excitation energies. This is also reflected in the so-called "backbending plot" [twice the moment of inertia versus the square of the rotational frequency with $2\theta/\hbar^2$ and $(\hbar\omega)^2$ defined as in Ref. 12] for the yrast spectrum, which is presented in Fig. 7. The backbending is reproduced at exactly the right spin value and the overall shape of the experimental curve is also rather well described. As compared to the HFB cranking approach[18–20] up to now the only microscopic model which could be successfully applied to the backbending in rare-earth nuclei, the MONSTER method yields obviously a more quantitative description (see, for example, the cranking result for ^{162}Er in Ref. 20). This is especially true in the band-crossing region where the cranking approach because of the large and strongly varying angular momentum fluctuations contained in its wave functions runs into serious trouble.[21]

Another advantage of the MONSTER approach using quantum-mechanical many-body states having the proper symmetries as configuration space is that the resulting wave functions can be directly used to calculate also nondiagonal quantities like electromagnetic transition probabilities. As an example the calculated $B(E2)$ values in and in between the yrast and the yrare band are displayed in Fig. 8 and compared to the experimental data.[45–47] In the MONSTER calculation here the Kumar-Baranger values for the effective charge[23] ($e_p=1.622e, e_n=0.622e$ have been taken. The agreement with the experimental data is rather satisfactory and could be even further improved if, as could be easily justified because of our smaller single-particle basis, slightly larger effective charges would be used. Further information about the $E2$ properties of the yrast and yrare bands can be found in Table V, where the usual rotational limit has been used to extract from the calculated spectroscopic quadrupole moments and $B(E2)$ values the static and dynamic intrinsic quadrupole moments $Q_0(I)$ and $Q^{\rm dyn}_{I;I-2}$, respectively.

Obviously, the MONSTER does not only yield the yrast and yrare levels but produces a lot of other excited states, too. As an example the calculated γ band is compared

TABLE V. Dynamic quadrupole moments $Q^{\rm dyn}_{I;I-2}$ as calculated from the $B(E2;I\to I-2)$ values and spectroscopic quadrupole moments $Q_0(I)$ in ^{164}Er. In the rotational limit both these quantities should be constant with I. Columns labeled with "yrast" refer to the yrast, those with "yrare" to the yrare band. For the dynamical moments also the cross terms "yrast yrare" and "yrare yrast" are given. As effective charges the Kumar-Baranger (Ref. 23) values $e_p=1.622e$ and $e_n=0.622e$ have been taken.

	$Q^{\rm dyn}_{I;I-2}/e$ fm^2				$Q_0(I)/e$ fm^2	
$I/\hbar$	yrast	yrare	yrast→ yrare	yrare→ yrast	yrast	yrare
2	712				711	
4	713				707	
6	714				700	
8	718				696	
10	720				688	672
12	719	582	79	55	684	655
14	701	651	165	164	684	642
16	525	499	464	489	669	652
18	665	671	194	224	659	661
20	689	705	53	75	656	660
22	690	706	21	39		

with the experimental one[45] in Fig. 9. In addition to the excitation energies here also the $B(E2)$ values (in units of e^2fm^4) are displayed. It is easily seen that though the overall qualitative features of the experimental γ band can be reproduced, the quantitative description of the spectrum is far less accurate than in the case of the yrast and yrare bands especially for the higher spin states. Furthermore, in order to reproduce the experimental 2^+ bandhead energy the theoretical spectrum had to be shifted down by 640 keV. Thus obviously the present MONSTER calculations for ^{164}Er should still be improved.

There are several possibilities to achieve this. For example, in future calculations the full Kumar-Baranger basis ($N=4,5$ for protons, $N=5,6$ for neutrons) should be taken. Furthermore, it is intended to enlarge the number of configurations and such to improve the description especially of the side bands. In addition it is by no means obvious that the effective interaction should have the simple structure assumed here. More realistic effective forces may be necessary. Lastly, in order to find a reasonable parametrization of such interactions and also to get some experience about how many 2qp excitations should be included in the configuration space, definitely a systematic study of several nuclei in the rare-earth region will be unavoidable. Such a systematic investigation will be done in the near future.

Nevertheless, we think already that the present calculations for ^{164}Er prove the ability of the MONSTER approach to describe not only light and medium heavy nuclei but also the backbending effect and the related phenomena observed in the rare-earth region.

Finally, before closing this section, we would like to mention that the MONSTER code though doing a tremendous job is far less time consuming than one would expect. So, for example, the calculation of all the energies and wave functions in the ^{20}Ne and ^{22}Ne cases took 1.5 and 2.5

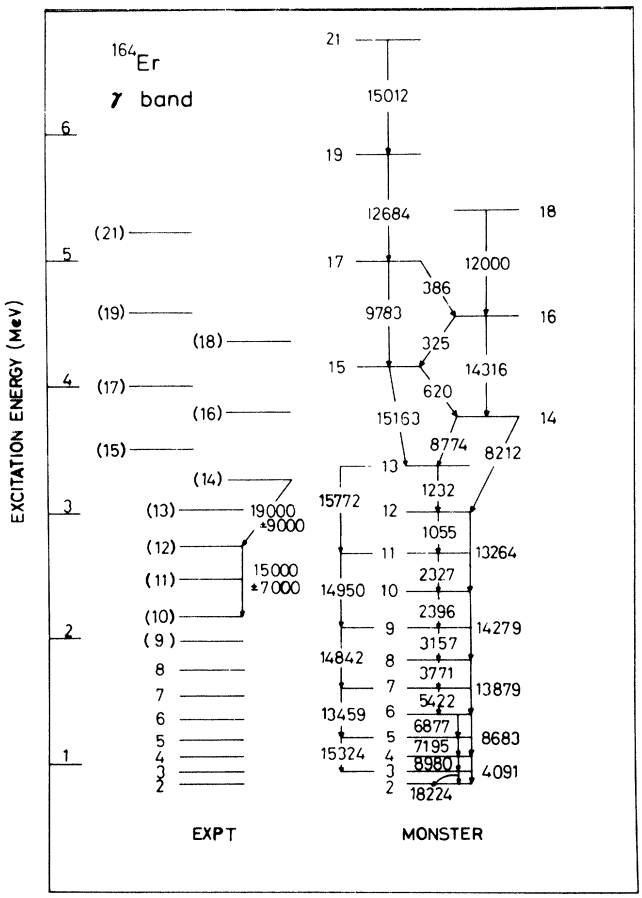

FIG. 9. γ band of ^{164}Er is displayed. The experimental data have again been taken from Ref. 45. The MONSTER results have been renormalized to the experimental band head energy (downshift of 640 keV). In addition various $B(E2)$ values, all in units of e^2fm^4, are given.

min CPU time, respectively. The ^{46}Ti was the most time consuming example. Here 2 h of CPU time were needed. The ^{164}Er calculation, on the other hand, was done in only about 1.5 h CPU. All these times are measured on the Tübingen Univac 1100/80. On the Jülich IBM the code runs by a factor of more than 4 faster.

V. CONCLUSIONS

The MONSTER approach discussed in the present paper approximates the nuclear wave functions by linear combinations of the angular momentum and number projected HFB vacuum and the corresponding equally spin and number projected 2qp excitations with the configuration mixing degrees of freedom to be determined after the required symmetry properties of the quasiparticle determinants have been restored. Thus the model accounts for possible spin dependencies of the configuration mixing and simultaneously avoids all the difficulties due to rotational spurious admixtures which would occur if the chosen Hamiltonian would be diagonalized in spin-nonconserving configuration spaces. The MONSTER can be considered as a straightforward extension of the spin projected particle hole model (PHM) on HF basis, which has been used during the last couple of years with some success for the description of giant multipole resonances as well as of low excited states in self-conjugate light doubly even nuclei.[11,13–15] Hence it contains all the advantages of the latter. However, accounting in addition for the rather important proton-proton and neutron-neutron pairing correlations by taking an HFB instead of an HF reference potential, the MONSTER can be applied to a much larger variety of nuclear structure problems than the simpler PHM approximation.

The MONSTER computer code developed during the last three years allows for rather general applications. So, for example, large single-particle and configuration spaces can be used as well as arbitrary two-body forces. Unlike a similar method recently presented by Hara,[48] who neither allows for general two-body forces nor projects on the proper particle numbers, the MONSTER is not restricted to rather special nuclear structure problems but can be applied almost anywhere in the mass table. Furthermore, besides the low excited states in not too heavy nuclei also higher excitations like the giant multipole resonances are numerically accessible. Lastly, besides the energies and wave functions the MONSTER code allows also the calculation of electromagnetic transitions and transition probabilities of various multipolarities ($L^{\pi} \leq 10^{\pm}$) and hence a very detailed analysis of the wave functions.

In the present paper several applications of the MONSTER have been discussed. First, it has been shown that in small model spaces the MONSTER wave functions are a rather good approximation to those resulting from a complete shell model diagonalization (SCM). As examples spectra and $B(E2)$ values for the two nuclei ^{20}Ne and ^{22}Ne obtained in a $1s\,0d$ shell basis have been presented. Second, using the full $1p\,0f$ basis the nucleus ^{46}Ti has been studied. Here the MONSTER turned out to be superior to a couple of other microscopic approaches and a rather satisfying agreement with the experimental data could be achieved. Finally, the MONSTER has been applied to the nucleus ^{164}Er. Though only a rather simple *ad hoc* chosen interaction was used, here the agreement with the experimental data is rather encouraging. So, for example, the excitation energies of both the ground as well as the S-band levels could be very well reproduced and also for the $B(E2)$ values the agreement with the experimental data is rather satisfying. Problems do still exist with the description of some side bands like the γ band. However, here the use of a more realistic interaction and a larger basis and configuration space is likely to improve the results considerably.

We believe that the results presented here provide convincing evidence for the applicability of the MONSTER in various mass regions. Obviously there is still a lot to be done. Many systematic studies will be needed to find out how the effective interactions to be used in different model spaces and mass regions should look like and what particular configuration spaces have to be used. Furthermore, in the long run it would obviously be desirable to improve the basic MONSTER assumptions in the direction of the more sophisticated models discussed in paper I of the present series of papers. One large step in this direction would be the use of a spin-dependent HFB transformation as reference for the MONSTER approach, another the inclusion of proton neutron pairing. Both steps would help to account for even more correlations in the nuclear wave functions than the present approach. Since they do not require any essentially new techniques besides those already used in the present MONSTER code, the numerical realization of these two steps seems to be possible within the next few years.

Thus at present we are at the beginning of a long road. Only the first steps have been taken. However, we are quite confident that the MONSTER may develop during the next few years into a rather useful tool for microscopic nuclear structure investigations in various mass regions, including light as well as intermediate and heavy nuclei.

[1]K. W. Schmid, F. Grümmer, and A. Faessler, preceding paper, Phys. Rev. C 29, 291 (1984).

[2]K. W. Schmid and F. Grümmer, in *Proceedings of the Nuclear Physics Workshop ICTP, Trieste, 1981,* edited by C. H. Dasso, R. A. Broglia, and A. Winther (North-Holland, Amsterdam, 1982), p. 161; in *Proceedings of the 1982 INS Symposium on Dynamics of Nuclear Collective Motion, Mt. Fuji,* edited by K. Ogawa and K. Tanabe (INS University of Tokyo, Tokyo, 1982), p. 188; A. Faessler (unpublished).

[3]K. W. Schmid, H. Müther, K. Goeke, A. Faessler, and F. Grümmer, Phys. Lett. 63B, 399 (1976).

[4]K. Hara and S. Iwasaki, Nucl. Phys. A332, 61 (1979); A348, 200 (1980).

[5]F. Grümmer, K. W. Schmid, and A. Faessler, Z. Phys. A300, 77 (1981).

[6]N. N. Bogoliubov, Zh. Eksp. Teor. Fiz. 34, 58 (1958) [Sov.

Phys.—JETP 7, 41 (1958)]; Usp. Fiz. Nauk. 67, 549 (1959) [Sov. Phys.—Usp. 2, 236 (1959)]; N. N. Bogoliubov and V. G. Soloviev, Dokl. Akad. Nauk. SSSR 124, 1011 (1959) [Sov. Phys.—Dokl 4, 143 (1959)]; J. G. Valatin, Phys. Rev. 122, 1012 (1961).

[7]H. H. Wolter, A. Faessler, and P. U. Sauer, Nucl. Phys. A167, 108 (1971).

[8]B. F. Bayman, Nucl. Phys. 15, 33 (1960).

[9]R. E. Peierls and J. Yoccoz, Proc. Phys. Soc. London, Sect. A 70, 381 (1957); F. Villars, in *Proceedings of the International School of Physics "Enrico Fermi", Course XXXVI,* edited by C. Bloch (Academic, New York, 1966), Vol. 36. p. 1.

[10]A. R. Edmonds, *Angular Momentum in Quantum Mechanics* (Princeton University Press, Princeton, 1957).

[11]K. W. Schmid and G. Do Dang, Phys. Rev. C 15, 1515 (1977); 18, 1003 (1978); K. W. Schmid, *ibid.* 24, 24 (1981).

[12]R. M. Lieder and H. Ryde, Adv. Nucl. Phys. 10, 1 (1978).

[13]K. W. Schmid and G. Do Dang, Z. Phys. A 276, 233 (1976).

[14]K. W. Schmid and H. Müther, Phys. Rev. C 16, 2050 (1977).

[15]K. W. Schmid and R. Smith, Nucl. Phys. A381, 195 (1982).

[16]J. P. Elliot and T. H. R. Skyrme, Proc. R. Soc. London Ser. A 323, 561 (1955).

[17]B. Giraud, Nucl. Phys. 71, 373 (1965).

[18]H. J. Mang, Phys. Rep. 18, 325 (1975).

[19]A. L. Goodman, Adv. Nucl. Phys. 11, 263 (1979).

[20]A. Faessler, M. Ploszajczak, and K. W. Schmid, Prog. Part. Nucl. Phys. 5, 79 (1980).

[21]I. Hamamoto, Nucl. Phys. A271, 15 (1976); F. Grümmer, K. W. Schmid, and A. Faessler, *ibid.* A306, 134 (1978); A308, 77 (1978).

[22]H. J. Mang, in *Proceedings of the 1982 INS Symposium on Dynamics of Nuclear Collective Motion, Mt. Fuji,* edited by K. Ogawa and K. Tanabe (INS University of Tokyo, Tokyo, 1982), p. 158.

[23]M. Baranger and K. Kumar, Nucl. Phys. A110, 490 (1968); A110, 529 (1968).

[24]H. J. Mang, B. Samadi, and P. Ring, Z. Phys. A279, 325 (1976); J. L. Egido, H. J. Mang, and P. Ring, Nucl. Phys. A334, 1 (1980).

[25]J. H. Wilkinson, *The Algebraic Eigenvalue Problem* (Clarendon, Oxford, 1965).

[26]E. Halbert, J. B. McGrory, B. H. Wildenthal, and S. P. Pandhya, Adv. Nucl. Phys. 4, 316 (1971).

[27]R. R. Whitehead, A. Watt, B. J. Cole, and I. Morrison, Adv. Nucl. Phys. 9, 123 (1977).

[28]A. Plastino, R. Arvieu, and S. A. Moszkowski, Phys. Rev. 145, 837 (1966); R. Arvieu and S. A. Moszkowski, *ibid.* 145, 830 (1966); P. W. M. Glaudemans, P. J. Brussaard, and B. H. Wildenthal, Nucl. Phys. A102, 593 (1967).

[29]The calculations have been performed by P. Rath, University of Tübingen.

[30]A. Arima, V. Gillet, and J. Ginocchio, Phys. Rev. Lett. 25, 1043 (1970); L. Satpathy, K. W. Schmid, and A. Faessler, *ibid.* 28, 832 (1972); L. Satpathy, K. W. Schmid, S. Krewald, and A. Faessler, Phys. Rev. C 14, 1995 (1976).

[31]T. T. S. Kuo and G. E. Brown, Nucl. Phys. A114, 241 (1968).

[32]J. B. McGrory, Phys. Rev. C 8, 693 (1973).

[33]H. Müther, K. Goeke, K. Allaart, and A. Faessler, Phys. Rev. C 15, 1467 (1977).

[34]W. Kutschera, B. A. Brown, and K. Ogawa, Riv. Nuovo Cimento 1, No. 12,1 (1978).

[35]L. D. Skouras, J. Phys. G 1, 438 (1975).

[36]W. Dehnhardt, O. C. Kistner, W. Kutschera, and H. J. Sann, Phys. Rev. C 7, 1471 (1973).

[37]J. L. Durell, G. D. Dracoulis, and W. Gelletly, J. Phys. A 12, 1448 (1974).

[38]R. L. Auble, Nucl. Data Sheets 24, 1 (1978).

[39]G. D. Dracoulis, D. C. Radford, and A. Poletti, J. Phys. G 4, 1323 (1978).

[40]N. R. F. Rammo, P. J. Nolan, L. L. Green, A. N. James, J. F. Sharpey-Schafer, and H. M. Sheppard, J. Phys. G 8, 101 (1982).

[41]N. V. De Castro Faria, J. Charbonneau, J. L'Ecuyer, and R. J. A. Levesque, Nucl. Phys. A174, 37 (1971).

[42]H. Müther (private communication).

[43]S. Siegel and L. Zamick, Nucl. Phys. A145, 89 (1970); K. W. Schmid and G. Do Dang, Z. Phys. 268, 65 (1974).

[44]O. C. Kistner, A. W. Sunyar, and E. der Mateosian, Phys. Rev. C 17, 1417 (1978).

[45]S. W. Yates, I. Y. Lee, N. R. Johnson, E. Eichler, L. L. Riedinger, M. W. Guidry, A. C. Kahler, D. Cline, R. S. Simon, P. A. Butler, P. Colombani, F. S. Stephens, R. M. Diamond, R. M. Ronnigen, R. D. Hichwa, J. H. Hamilton, and E. L. Robinson, Phys. Rev. C 21, 2366 (1980).

[46]I. Ben-Zvi, A. E. Blaugrund, Y. Dar, G. Goldring, J. Hess, M. W. Sachs, E. Z. Skurnik, and Y. Wolfson, Nucl. Phys. A117, 625 (1968).

[47]F. Kearns, G. Vorley, G. D. Dracoulis, T. Inamura, J. C. Lisle, and J. C. Wilmott, Nucl. Phys. A278, 109 (1977).

[48]K. Hara, in *Proceedings of the 1982 INS Symposium on Dynamics of Nuclear Collective Motion, Mt. Fuji,* edited by K. Ogawa and K. Tanabe (INS University of Tokyo, Tokyo, 1982), p. 158.